



Hydration States and Blood Compatibility of Hydrogen-Bonded Supramolecular Poly(2-methoxyethyl acrylate)

Jankova, Katja; Javakhishvili, Irakli; Kobayashi, Shingo; Koguchi, Ryohei; Murakami, Daiki; Sonoda, Toshiki; Tanaka, Masaru

Published in:
Acs Applied Bio Materials

Link to article, DOI:
[10.1021/acsabm.9b00363](https://doi.org/10.1021/acsabm.9b00363)

Publication date:
2019

Document Version
Peer reviewed version

[Link back to DTU Orbit](#)

Citation (APA):

Jankova, K., Javakhishvili, I., Kobayashi, S., Koguchi, R., Murakami, D., Sonoda, T., & Tanaka, M. (2019). Hydration States and Blood Compatibility of Hydrogen-Bonded Supramolecular Poly(2-methoxyethyl acrylate). *Acs Applied Bio Materials*, 2(10), 4154-4161. <https://doi.org/10.1021/acsabm.9b00363>

General rights

Copyright and moral rights for the publications made accessible in the public portal are retained by the authors and/or other copyright owners and it is a condition of accessing publications that users recognise and abide by the legal requirements associated with these rights.

- Users may download and print one copy of any publication from the public portal for the purpose of private study or research.
- You may not further distribute the material or use it for any profit-making activity or commercial gain
- You may freely distribute the URL identifying the publication in the public portal

If you believe that this document breaches copyright please contact us providing details, and we will remove access to the work immediately and investigate your claim.

1
2
3
4
5
6
7 Hydration states and blood compatibility of
8
9
10
11 Hydrogen-bonded supramolecular poly(2-
12
13
14
15 methoxyethyl acrylate)
16
17
18
19

20 *Katja Jankova,^{1,2} Irakli Javakhishvili,³ Shingo Kobayashi,¹ Ryohei Koguchi,^{1,4} Daiki*

21
22
23
24 *Murakami,¹ Toshiki Sonoda,¹ and Masaru Tanaka^{1*}*
25
26
27

28
29 ¹ Soft Materials Chemistry, Institute for Materials Chemistry and Engineering, Kyushu
30
31
32 University, Build. CE41, 744 Motooka Nishi-ku, Fukuoka, 819-0395, Japan
33
34
35

36
37 ² Department of Energy Conversion and Storage, Technical University of Denmark,
38
39
40 Elektrovej, Build. 375, 2800 Kongens Lyngby, Denmark
41
42
43

44
45 ³ Danish Polymer Centre, Department of Chemical and Biochemical Engineering,
46
47
48 Technical University of Denmark, Build. 229, 2800 Kongens Lyngby, Denmark
49
50
51
52
53
54
55
56
57
58
59
60

1
2
3
4 ⁴ AGC Inc. New Product R&D Center, 1150 Hazawa-cho, Kanagawa-ku, Yokohama,
5
6
7 Kanagawa 221-8755, Japan
8
9
10

11 KEYWORDS: blood compatible polymer, hydrogen bonding, poly(2-methoxyethyl
12
13
14
15 acrylate), free-standing film, intermediate water, 2-{3-(6-methyl-4-oxo-1,4-
16
17
18 dihydropyrimidin-2-yl)ureido}ethyl methacrylate.
19
20
21
22
23
24
25
26
27

28 ABSTRACT: The practical use of the viscous liquid polymer, poly(2-methoxyethyl
29
30
31 acrylate) (PMEA) was expanded from thin films with excellent blood compatibility to
32
33
34 thick coatings and free-standing films without essentially sacrificing its blood
35
36
37 compatibility. This was undertaken by creating multiple hydrogen-bonding polymer
38
39
40 networks by introducing a functional methacrylic monomer bearing a 6-methyl-2-ureido-
41
42
43 4[1H]-pyrimidone group in the PMEA backbone via free radical copolymerization. The
44
45
46 hydrogen-bonded PMEA (H-PMEA) contained about 6 mol% of the functional monomer
47
48
49 in the copolymer. These functional monomers as physical cross-links are distributed in
50
51
52
53
54
55
56 the PMEA matrix with a T_g of -35 °C, making H-PMEA solid rubber-like material with
57
58
59
60

1
2
3 recoverable tensile strain. Additionally, mechanical tests revealed its tensile strength,
4
5
6
7 and thermogravimetric analyses confirmed its higher thermostability. The dry and
8
9
10 hydration states of H-PMEA were assessed by differential scanning calorimetry, contact
11
12
13 angle, and atomic force microscopy measurements. Comparison with viscous PMEA was
14
15
16 made. For the first time, we included PVC alongside with PET, the surface we usually
17
18
19 use as a negative control, in the platelet adhesion test with human blood, and found out
20
21
22 that 1.5 times more platelets adhered onto the PVC surface than onto the PET surface,
23
24
25
26 while H-PMEA proved to have a clear edge. Thus, H-PMEA may serve as a suitable
27
28
29 replacement of polymers in products contacting blood as it shows potential for making
30
31
32 free-standing films, thick coatings, implants and articles with various geometries for the
33
34
35
36
37
38 medicinal industry.
39
40
41
42
43
44
45
46
47
48
49
50
51
52

53 Introduction

54
55
56
57
58
59
60

1
2
3
4 Compatibility with human blood is an important characteristic of materials used in
5
6
7 medical devices. Poly(2-methoxyethyl acrylate) (PMEA) is an acrylic homopolymer
8
9
10 having an ethylene oxide unit in the side chain. It has low toxicity and is FDA approved
11
12
13
14 for medical use. This polymer boasts the largest share on coating market, is easy to
15
16
17 synthesize and inexpensive, possesses excellent blood compatibility, low protein
18
19
20 adsorption and denaturation.¹⁻³ Intermediately hydrophilic, with the water contact angle
21
22
23
24 of approximately 40 degrees, it is not soluble in water above the molecular weight (MW)
25
26
27 of 4-5 kDa, but it is soluble in methanol as well as many other organic solvents. Being a
28
29
30
31 viscous liquid has not obstructed PMEAs extensive use, especially in the Japanese
32
33
34 industry, to coat various organic and inorganic surfaces to which the polymer adheres
35
36
37 well. These properties made it very useful to coat with a thin film of liquid PMEA various
38
39
40
41 stents, an artificial oxygenator,⁴ a bioartificial liver, heart,⁵ cell enrichment filter, etc., and
42
43
44 thus to protect blood from contacting the substrate material. However, only thin films
45
46
47 were possible to be produced from PMEA so far. When the thickness of the film is
48
49
50 below 50 microns the films are not sticky. Usually, for coating purposes, PMEA with the
51
52
53 number average MW of around 23,000 Da (18-25 kDa) has been used.¹⁻³ The effect of
54
55
56
57
58
59
60

1
2
3 the MW of PMEA on the interfacial structure and the blood compatibility was
4
5
6 investigated very recently.⁶ PMEAs with higher MWs were found to have a very little (30
7
8 and 44 kDa) or even more (183 kDa) reduced blood compatibility as compared to PMEA
9
10
11 with 19 kDa. These PMEAs with higher MW were also viscous and sticky. Recently,
12
13
14 charged PMEA microspheres were synthesized⁷ by aqueous precipitation
15
16
17 polymerization with potassium peroxydisulfate, and were also turned into small free-
18
19
20
21
22
23
24 standing films with thicknesses up to 1.2 mm.
25
26
27

28 Liquid polymers can be transformed into higher viscosity products by using either
29
30
31 chemical or physical cross-linking. The chemical crosslinks are introduced by curing
32
33
34 where covalent bonds are formed. However, besides using an additional step of curing,
35
36
37 the material cannot be processed afterwards. Non-covalent interactions are often the
38
39
40
41 means of property improvement in polymer science. By introducing hydrogen bonding,
42
43
44 metal complexation, ionic or hydrophobic interactions, etc. the supramolecular polymer,
45
46
47 which can be recycled, is obtained.⁸⁻⁹ Hydrogen bonding is not the strongest among the
48
49
50
51 non-covalent interactions, but has been employed to confer many new functionalities
52
53
54 like stimuli-responsiveness¹⁰ and self-healing properties to polymeric materials.¹¹⁻¹⁴
55
56
57
58
59
60

1
2
3
4 Acid-base interactions are often utilized in polymer electrolyte membranes for fuel cells
5
6
7 to increase the strength and conductivity of the ionic polymers.¹⁵⁻¹⁷ We have previously
8
9
10 exploited a strategy involving hydrophobic interactions both in aq. solutions¹⁸⁻¹⁹ and in
11
12
13 bulk.²⁰ Triblock copolymers with small amounts of outer blocks were designed, which
14
15
16 could associate in bulk to build a morphology very similar to that of the thermoplastic
17
18
19 elastomers, where hard segments act as physical cross-links distributed in a matrix of a
20
21
22 low T_g polyether polymer – this way Li ion conducting solid polymer electrolytes
23
24
25 comprising PEG or PEG/PEGPG soft segments together with polyethylene or
26
27
28 polypentafluorostyrene hard segments could be produced.²⁰⁻²¹
29
30
31
32
33

34
35 Introducing additional chemical or physical interactions in MEA would allow
36
37
38 preparation of a solid PMEA, which in turn would make it possible to manufacture thick
39
40
41 coatings and materials with various shapes without negatively affecting its blood
42
43
44 compatibility. Since the mid-20th century, plasticized PVC has been utilized to collect
45
46
47 and store whole blood, and various blood bags, tubes, catheters, etc. have been
48
49
50 produced. Usually, the sodium salt of citric acid is added to the blood²² acting as an
51
52
53 anticoagulant, and increasing the stability of blood with time. As the most harmful in
54
55
56
57
58
59
60

1
2
3
4 PVC are plasticizers, new plasticizers other than phthalates (including citrates) are
5
6
7 being employed.²²⁻²⁶ Polymers other than PVC are being developed as well.²³⁻²⁴
8
9
10 However, both new plasticizers and polymers are expensive. Additionally, some of the
11
12
13
14 new plasticizers for PVC have a foul odour, cause allergic reactions and are
15
16
17 leachable.²⁵ Due to these drawbacks, alternative materials are constantly sought.
18
19
20
21 RENOLIT *Medical* supplies polyolefins,²³ while MELITEK provides *XE film grades* of PP
22
23
24 with high purity and without plasticizers for medical and pharmaceutical applications.²⁴ It
25
26
27 is claimed that these non-PVC containing alternatives fulfil all the demands posed on
28
29
30
31 blood compatible materials. However, these alternative solutions are not economical.

32
33
34
35 The goal of this work is to combine benefits of PVC and PMEA into a single platform
36
37
38 in an attempt to mitigate the problem associated with the scarcity of materials suitable
39
40
41 for blood-contacting applications. Thus, a strategy to convert the low viscosity and
42
43
44 highly blood compatible PMEA into a solid polymer without substantially decreasing its
45
46
47 blood compatibility by employing copolymerization of MEA with a strong hydrogen-
48
49
50 bonding monomer in a simple and facile manner is proposed.
51
52
53
54
55
56
57
58
59
60

Experimental

Materials

The MEA monomer (Sigma-Aldrich) was passed through a pre-packed disposable column to remove an inhibitor. α,α' -Azobis(isobutyronitrile) (AIBN) was recrystallized from methanol. All other solvents or chemicals were employed as received unless specified otherwise. PVC was kindly supplied from Sekisui co., Japan. AIBN and phosphate-buffered saline (PBS) were obtained from FUJIFILM Wako Pure Chemical Corporation, Japan. Bovine serum albumin (BSA) and human fibrinogen from Sigma-Aldrich, USA, and human whole blood for the platelet adhesion test from Tennessee blood services, USA were employed. The micro-BCA protein assay kit from Thermo Fisher Scientific, USA was used to evaluate the amount of adsorbed protein.

Synthesis and molecular characteristics of polymers

PMEA was prepared by free radical polymerization. The polymerization was conducted in 1,4-dioxane at 75 °C for 6 hours making use of AIBN as the initiator.²⁷⁻²⁸ The polymer was precipitated from THF/hexane mixture, and dried *in vacuo* at 60 °C for several days. The functional 2-{3-(6-methyl-4-oxo-1,4-dihydropyrimidin-2-yl)ureido}ethyl methacrylate and its H-bonding copolymer with MEA (H-PMEA) were synthesized and analyzed as reported in the literature.²⁹ H-PMEA copolymer prepared in this work contains 6 mol% of the functional monomer according to ¹H NMR spectroscopy (Figure S1). The molecular weight characteristics of both polymers are presented in Table 1.

Table 1. Glass transition temperatures, static water contact angles and the molecular weight characteristics of the synthesized PMEA, H-PMEA, and the used PET substrate

Polymer	$T_{g \text{ dry,}}$ °C	$T_{g \text{ hydrated,}}$ °C	M_n^b Da	M_w/M_n	Sessile drop 30 s	Captive bubble 30 s
PMEA	-35.0	-50.1	22,000	2.81	42 ± 2	133 ± 2
H-PMEA	-33.3	-41.5	25,800	2.13	65 ± 2	142 ± 1
PET	76	-	-	-	80 ± 1	115 ± 3

^a Measurements (degree, mean ± SD, n=5) of the polymer films (annealed overnight at 60 °C)

^b Determined by SEC with a PS calibration curve

Analyses

Analytical techniques

¹H NMR spectra were acquired on JEOL 500 MHz JNM-ECX and Bruker Avance 300 MHz spectrometers in DMSO-*d*₆ or CDCl₃ at room temperature.

Molecular weights and polydispersity indices were estimated by Size-Exclusion Chromatography (SEC) equipped with a triple detector array (refractive index, right

1
2
3 angle laser light scattering, and viscometer) SEC system of Malvern Viscotek TDAmx
4
5
6 and Tosoh TSKgel columns connected in a series of guard column H_{HR}-H, GMH_{HR}-H
7
8
9
10 × 2, and G2000H_{HR}. Measurements were carried out in THF at 40 °C with a flow rate of
11
12
13
14 1.0 mL/min. The system was calibrated using narrow molecular weight distribution PS
15
16
17 standards in the range of $5 \times 10^2 - 3.64 \times 10^5$ g/mol.
18
19
20

21 Differential scanning calorimetry (DSC) measurement was conducted in the
22
23
24 temperature range of -100-50 °C and at the rate of 5.0 °C/min on a Seiko Instruments
25
26
27 Inc. X-DSC7000 purged with N₂. T_g was determined from the second heating curve
28
29
30
31 automatically, and is reported as the onset of the thermal transition. A TGA Q500
32
33
34 apparatus from TA Instruments was utilized to conduct thermogravimetric analyses
35
36
37
38 (TGA). Samples were heated from 20 to 550 °C with a heating rate of 5 °C/min under
39
40
41
42 either air or nitrogen flow.
43
44
45
46
47

48 *Mechanical tests*

49
50
51 Films of H-PMEA and PVC with a thickness of 0.1 - 0.2 mm were hot pressed from each of
52
53
54 the polymers between 2 PTFE plates first at 60 °C for 15 min under a pressure of 5 MPa, and at
55
56 150 °C for 15 min at 10 MPa, respectively, and then 5 more minutes at room temperature.
57
58
59
60

Polymer films were drawn uniaxially at a rate of 10 mm/min with a universal tensile testing machine (Tensilon RTC-1210A, A&D Co., Ltd.) at room temperature. Dogbone specimens 64 mm long and 10 mm broad were used, and the measuring part was 10 mm long.

Quantification of water-polymer interactions

In hydrated macromolecules, 3 kinds of water are determined:^{27,28,30} non-freezing water (*NFW*), intermediate water (*IW*), and free water (*FW*), and their content is given as *NFWC*, *IWC*, and *FWC*, respectively. DSC is employed to estimate the equilibrium water content (*EWC*) of a polymer as the water content at which a peak at about 0 °C corresponding to the melting of ice and a small shoulder or peak below this temperature originating from melting of *IW* appear, and is given in equation (1):

$$\text{EWC (wt\%)} = ((W_1 - W_0) / W_1) \times 100 \quad (1)$$

where W_0 and W_1 are the weight of the dry and hydrated sample, respectively.

In hydrated polymers, *EWC* encompasses different types of water as expressed by equation (2):

$$\text{EWC (wt\%)} = \text{NFW (wt\%)} + \text{IW (wt\%)} + \text{FW (wt\%)} \quad (2)$$

$$\text{IW (wt\%)} = \Delta H_{cc} / 334(\text{Jg}^{-1}) \quad (3)$$

$$\text{FW (wt\%)} = (\Delta H_m / 334(\text{Jg}^{-1})) - \text{IW} \quad (4)$$

ΔH_{cc} represents enthalpy change during cold crystallization whereas ΔH_m is enthalpy change during the melting of ice. 3-7 mg of samples was taken. Before measurements, the samples were immersed in ultrapure water for 7 days to attain full hydration.

1
2
3 *Preparation and characterization of the polymer surfaces*
4

5 Film samples were produced and utilized for contact angle (CAs) and atomic force microscopy
6 (AFM) measurements as well as for the human blood platelet adhesion test. For this reason, the
7
8 polymer samples H-PMEA and PMEA were dissolved in toluene (60 °C for 3 days) or methanol,
9
10 respectively, to give 0.2 wt/vol% solutions. Round-shaped PET surfaces with the diameter of 14
11
12 mm were washed with methanol, and the filtered polymer solutions were spin-coated onto them.
13
14 A Mikasa spin coater MS-A100 was used to coat the substrates in the following manner: Any
15
16 particular polymer solution was coated twice onto a substrate at rates of 500 rpm for 5 s, 2000
17
18 rpm for 10 s, slope for 5 s, 4000 rpm for 5 s, and slope for 4 s. Afterwards, the substrates were
19
20 dried at room temperature.
21
22
23
24
25

26 Water CAs on the airside of the polymer films were measured by the sessile drop
27
28 method with an accuracy of $\pm 2^\circ$ at 25 °C. An air bubble of 2 μL was injected to the
29
30 hydrated surface immersed in water in the captive bubble method, which is a means of
31
32 measuring the contact angle between a liquid and a solid by the drop shape
33
34 analysis.^{31,32} The averages of three measurements carried out at different positions of a
35
36 film are reported for both measurements.
37
38
39
40
41
42
43
44
45

46
47 AFM observations were carried out with a Bioscope Resolve (Bruker) Instrument with
48
49 a cantilever SNL-10 (spring constant $k = 0.35 \text{ N/m}$, resonance frequency $f = 65 \text{ kHz}$ in
50
51 air, tip radius $< 12 \text{ nm}$; Bruker). AFM topographies were imaged in PBS in a Peak Force
52
53
54
55
56
57
58
59
60

1
2
3 Tapping mode after the samples had been immersed in PBS for 60 min or longer. The
4
5
6
7 arithmetical mean height is determined before and after immersion in PBS for 60
8
9
10 minutes.
11
12
13
14
15
16

17 *Determination of the Amount of Adsorbed Protein by μ BCA and ELISA*^{1-3,27,28,30,31}
18
19
20

21 Amounts of the platelet poor plasma (PPP) adsorbed on the polymer surfaces were
22
23
24 quantified by the μ BCA. In addition, the ELISA was executed to relatively evaluate the
25
26
27
28 conformational alteration of the adsorbed fibrinogen from PPP.
29
30

31 The polymer surfaces for the μ BCA and the ELISA were prepared as follows: a 96-well
32
33 polypropylene plate was coated with the polymers by applying 15 μ L of the polymer solution
34
35 (0.2 wt/vol%) of PME A in methanol or of H-PME A in toluene, and slowly air-drying the surface
36
37 at room temperature for 3 days.
38
39

40 For both methods, 100 μ L of PBS was introduced in each well followed by incubating the
41
42 plate for 1 hour at 37 °C. The PBS was removed, 50 μ L of PPP was put on in each well, and the
43
44 plate was incubated again for another hour at the same temperature. PPP was removed from each
45
46 well, and the wells were rinsed with 200 μ L PBS for at least five times. In case of the μ BCA, a
47
48 30 μ L solution of 5% sodium dodecyl sulfate and 0.1 N NaOH was used to extract the adsorbed
49
50 proteins by incubation for 2 hours at 37 °C. The proteins were then evaluated by the μ BCA assay
51
52
53
54
55
56
57
58
59
60

1
2
3 following the manufacturer's instructions. The protein amount was determined by making use of
4 the albumin standard curve that had been prepared for each experiment.
5
6

7
8 When the ELISA was applied the procedure, in the beginning was the same as above
9
10 using PPP. The samples were then incubated with Blocking-One (Nacalai Tesque) for
11
12 30 min at the same temperature preventing non-specific reactions. Washing five times
13
14 with 200 μ L PBS as before followed. Further incubation with 50 μ L of Anti-Fibrinogen γ '
15
16 conjugated anti-mouse Immunoglobulin G (IgG) Ab for 2 hours at 37 $^{\circ}$ C followed. Lastly,
17
18 the samples were incubated with 2,2'-azinobis(3-ethylbenzothiazoline-6-sulfonic
19
20 acid)ammonium salt in a buffer (Roche Diagnostics). A plate reader (BIO-RAD) was
21
22 used to measure absorbance at a wavelength of 405 nm. The averages of 5
23
24 measurements are reported.
25
26
27
28
29
30
31
32
33
34
35
36
37
38
39
40
41
42
43
44
45
46

47 *Human Platelet Adhesion Test*^{1-3,27,28,30,31}

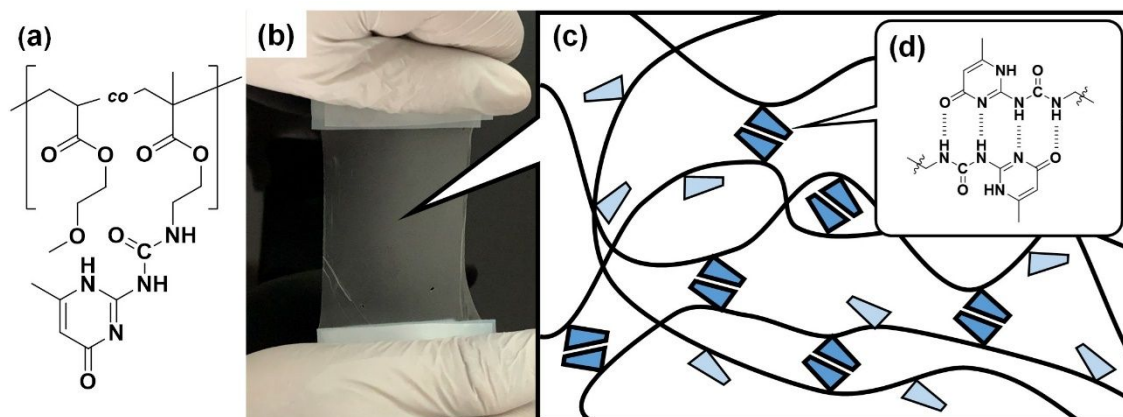
48
49

50 The polymer substrates for the platelet adhesion test with human blood were
51
52 fabricated in the following manner: 8 \times 8 mm squares were cut out of the polymer
53
54
55
56
57
58
59
60

1
2
3 coated substrates, and were mounted on an SEM specimen stage with a double-sided
4
5
6
7 tape. Platelet-rich plasma (PRP) and PPP were separated from human blood by
8
9
10 centrifuging in two stages: the first stage involved centrifuging at 1500 rpm for 5 min to
11
12
13 get PRP while the second stage involved centrifuging the same blood at 4000 rpm for
14
15
16
17 10 min to get PPP. The cells in PRP and PPP were counted on a hemocytometer, and a
18
19
20 plasma solution comprising 4×10^7 cells cm^{-2} of platelets was obtained by mixing the
21
22
23 PRP and PPP solutions in a predetermined ratio. 200 μL of the final solution was
24
25
26
27 applied onto the polymer-coated substrates, which afterwards were washed with PBS
28
29
30
31 twice. Immersion in 1% glutaraldehyde in PBS for 120 min at 37 °C ensured fixation of
32
33
34 the adhered platelets. As the final step, the substrates were washed in this order: once
35
36
37
38 with PBS, once with PBS-water 1:1 mixture, and twice with pure water. The substrates
39
40
41
42 were examined with SEM to determine the number of adhered platelets. Human blood
43
44
45 obtained from 3 different donors was used, and the platelet adhesion test was carried
46
47
48
49 out 3 times for statistical purpose. The averages of 5 points measured on 3 different
50
51
52 films are reported.
53
54
55
56
57
58
59
60

Results and discussion

A copolymer of MEA with the functional methacrylic monomer 2-{3-(6-methyl-4-oxo-1,4-dihydropyrimidin-2-yl)ureido}ethyl methacrylate^{8,9,33} was synthesized as reported by Shabir et al.²⁹ The copolymer contained about 6 mol% of the functional monomer as judged by ¹H NMR (Figure S1). The structure of the copolymer is depicted also in Scheme 1a. Because of the multiple hydrogen bonding, the copolymer was designated as hydrogen-bonding PMEAs (H-PMEAs). This kind of bonding between the copolymer chains is realized through strongly associating stickers (Scheme 1c and 1d). Introducing such stickers turns liquid PMEAs into solid, rubber-like, and not sticky H-PMEAs, which can be processed into a transparent self-supporting film shown in Scheme 1b. Films of various thicknesses can be produced by pressing the material at 60 °C and 5 MPa, or by solvent casting.



Scheme 1. Chemical structure of poly[2-methoxyethyl acrylate-co-2-{3-(6-methyl-4-oxo-1,4-dihydropyrimidin-2-yl)ureido}ethyl methacrylate] (H-PMEA) (a), appearance of the

1
2
3 polymer as a transparent self-supporting film (b), morphology with stickers (c), and
4
5
6
7 multiple hydrogen bonding at the side chains (d).
8
9

13 **Thermal and mechanical properties**

15 Besides being solid, H-PMEA features thermal stability. The overlay of the TGA curves of
16 PMEA and H-PMEA in air and nitrogen is shown in Figure S1. The initial degradation of H-
17 PMEA starts at around 30 °C later than that of PMEA, and it occurs in 2 steps. Having in mind
18 the high amount of water that is associated with the MEA polymers even in dry conditions it is
19 assumed that the process of dehydration for both polymers finishes at 300 °C. The second step is
20 related to the main degradation, where H-PMEA decomposes at a higher temperature than
21 PMEA. Thus, H-PMEA is more thermally stable than PMEA, a property gained by forming
22 physical cross-links.
23
24
25
26
27
28
29
30
31
32
33

34 For comparison, PVC degrades in 3 steps and at 300 °C already 45% to 50% of the polymer is
35 thermally decomposed.
36
37
38

39 The rheological properties of the copolymers of MEA and the functional methacrylic
40 monomer bearing a 6-methyl-2-ureido-4[1H]-pyrimidone group (3 or 8 mol% of the
41 functional monomer) have already been evaluated.²⁹ We investigate the basic
42 mechanical properties of the H-PMEA (with 6 mol% of the functional monomer)
43 synthesized for this work and PVC. Tensile stress measurements and DMA were
44
45
46
47
48
49
50
51
52
53
54
55
56
57
58
59
60

1
2
3 performed at room temperature. The film thickness was 0.1 and 0.2 mm for H-PMEA
4
5
6
7 and PVC, respectively. Big differences in the elastic modulus (0.3 and 220 PMA), tensile
8
9
10 stress (1.1 and 57.2 MPa), and elongation (814 and 8%) of H-PMEA and PVC films
11
12
13
14 were observed. The elastic modulus and the T_g of H-PMEA, determined by DMA are
15
16
17 close to those from the tensile stress and DSC measurements (Table 1). These results
18
19
20 show that although being of lower strength, H-PMEA is a rubber-like polymer, which can
21
22
23 be employed to form thick coatings. Furthermore, the acquired mechanical data confirm,
24
25
26
27 that this polymer is able to withstand the necessary loads for forming free-standing films
28
29
30
31 and articles, possibly with various forms and dimensions. The MW and the number of
32
33
34 hydrogen-bonding stickers in the H-PMEA can be adjusted further to obtain particular
35
36
37
38 target properties of the material.
39
40
41
42
43
44

45 Hydration structure of PME A and H-PMEA

46
47
48 The hydration structure of H-PMEA is evaluated by DSC, AFM, and contact angle
49
50
51 (CA) measurements, and compared to PME A with a similar MW (Table 1). The T_g of
52
53
54
55 both polymers in a dry state are quite close, however, they differ a lot in the hydrated
56
57
58
59
60

1
2
3 state. That PMEAs exhibit 15 °C lower T_g in its hydrated state is already known. It is
4
5
6
7 related to the polymer-water interactions that will be elaborated later in this paragraph.
8
9
10 T_g of H-PMEA in a hydrated state has decreased by only 8 °C – the hydrogen bonding
11
12
13
14 and thereby lower mobility restrict the diffusion of water, and therefore its interaction
15
16
17 with the high viscosity polymer is weakened. However, the T_g of the copolymer is still
18
19
20 below room temperature, –33.5 °C.
21
22
23

24 The CA measurements show that the intermediately hydrophilic PMEAs are transformed
25
26
27 into an intermediately hydrophobic H-PMEA polymer (Table 1). While the water CA (by
28
29
30 sessile drop method) is stable in case of PMEAs (42°), it continues changing with time
31
32
33 and from 65° at 30 min reaches 58° at 60 min for H-PMEA. The air CA (by captive
34
35
36 bubble method) is stable for both polymers and decreases from 142 to only 140° for H-
37
38
39
40
41
42
43
44
45
46
47
48
49
50
51
52
53
54
55
56
57
58
59
60
PMEAs during the 60 min scan – this polymer needs longer time to form its interfacial
structure with water. However, after immersing 24 hours in water there is no more
change in the air CA of H-PMEA. All these show that the copolymerization and the
physical cross-links have turned PMEAs into more hydrophobic H-PMEAs with lower
mobility – a feature responsible for the platelet adhesion onto a polymer.

1
2
3
4 Based on its interactions with a polymer, 3 kinds of water in macromolecules are
5
6
7 classified: non-freezing water (*NFW*), intermediate water (*IW*), and free water (*FW*). In
8
9
10 this order the polymer-water interactions decrease, and therefore also the freezing
11
12
13 bound water is referred to as *IW* as it has an intermediate association with the polymer
14
15
16 matrix. It is believed, that polymer's blood compatibility is related to the amount of *IW*.
17
18
19
20
21 The water content of both polymers is therefore investigated by DSC, and the results
22
23
24 are summarized in Table 2. Additionally, the DSC curves are shown in Figure S2. In the
25
26
27 cooling scan, only the T_g of H-PMEA could be detected. In contrast, PMEA shows *IW*
28
29
30 already in the cooling scan, whereas in case of H-PMEA it is observed in the heating
31
32
33 scan and with much lower content. This behaviour is characteristic of polymers with
34
35
36 lower mobility. Moreover, EWC of H-PMEA is quite different from that of PMEA; in the
37
38
39 former, this amount is more than twice decreased as the physical cross-links lead to a
40
41
42 reduction in free volume and a reduction in the polymer chain mobility. This prevents
43
44
45 water from easily entering into the free volume of the polymer. More data presented in
46
47
48
49
50
51
52 Table 2 show that this has happened by decreasing primarily *FW* (by 90%) and *IW* (by
53
54
55 40%) in H-PMEA. The H-bonding present in the polymer matrix increases the
56
57
58
59
60

1
2
3 interactions between macromolecules and decreases those between water and the
4
5
6
7 polymer chains: *IW* and *NFW* predominate in PMEAs as compared to H-PMEA. This
8
9
10 influences *FW* as well, which is being 10 times less in H-PMEA than in PMEAs. The IWC
11
12
13 is also lower in H-PMEA as compared to the NFWC, possibly due to the added
14
15
16
17 interactions of its cross-links with water resulting in more *NFW*. These results are
18
19
20
21 expected to influence the platelet adhesion on the surface of H-PMEA too.
22
23
24
25
26
27

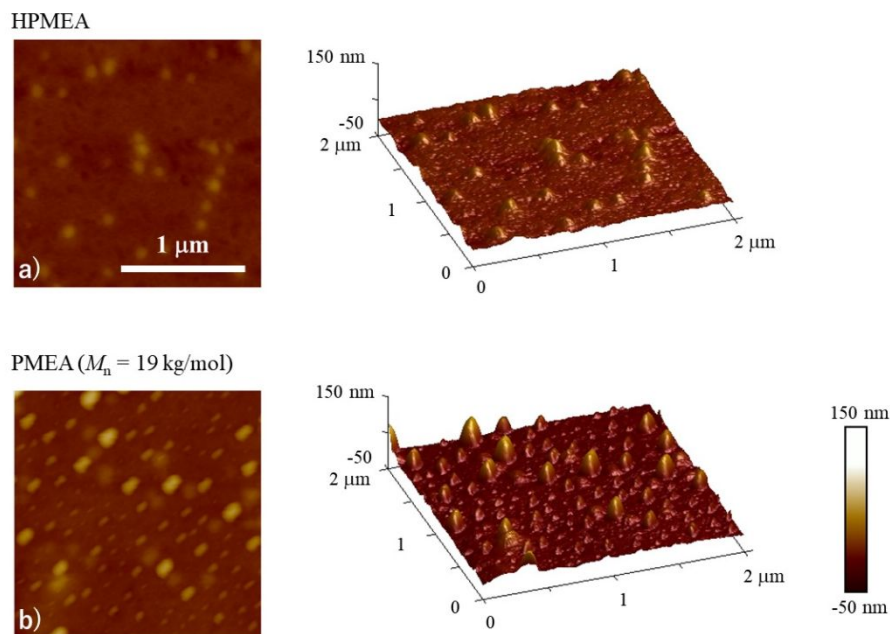
28 **Table 2.** Water content of the polymers
29
30
31

Polymer	EWC wt%	NFWC wt%	IWC wt%	FWC wt%	IWC/NFWC
PMEA	9.6	1.8	3.8	4.0	2.1
H-PMEA	4.3	1.6	2.3	0.4	1.4

46 **AFM of the hydrated polymers**

47
48
49 The interface morphology of the samples in dry and hydrated states was evaluated by
50
51
52
53 AFM. The AFM images of the dry polymers (not shown here), PMEAs³⁴⁻³⁶ and H-PMEA,
54
55
56
57
58
59
60

1
2
3 present flat structures with an arithmetical mean height around 5 nm. By immersing the
4
5
6
7 substrate with the polymers in PBS, continuous hydration of the surface induces phase
8
9
10 separation forming a nanoscale structure. Therefore, in the AFM images of the hydrated
11
12
13
14 polymers protrusions appear due to the micro-phase separation into polymer-rich and
15
16
17 water-rich domains.³⁴⁻³⁶ Such structures of polymer and water at the interfacial region
18
19
20 are characteristic for biopolymers containing a large amount of *W*. These interfacial
21
22
23
24 nanometer-scale structures in case of both investigated polymers have similar shapes
25
26
27 and are with similar domain sizes (Figure 1). The height of the protrusions for H-PMEA
28
29
30 has the same range as previously found for PMEAs: 50 - 80 microns.^{1-3,6,34-36} However,
31
32
33
34 the numbers of the soft protrusions/hills seem to be more and at the same time the
35
36
37 areas of the valleys are smaller in H-PMEA as compared to PMEAs, probably because of
38
39
40 these two being hydrophobic and hydrophilic, respectively. These facts resulted in the
41
42
43
44 less pronounced phase separation of H-PMEA clearly visible in its 2D and 3 D images.
45
46
47
48 The H-bonding obstructs segregation of the MEA polymer at the polymer-PBS interface,
49
50
51
52 which results in the possibility for the blood cells to settle down probably on the hills.³⁴⁻³⁶
53
54
55
56
57
58
59
60



24
25
26
27
28
29
30
31
32
33
34
35

Figure 1. Two- (left) and three-dimensional (right) images of the polymer/PBS interfaces of H-PMEA (a) and PMEa (b)

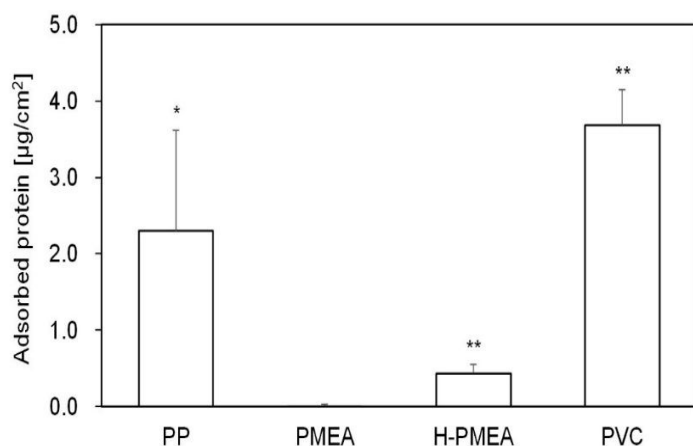
36
37
38
39
40
41
42

Protein adsorption and denaturation behavior on MEA polymers and negative control substrates

43
44
45
46
47
48
49
50
51
52
53
54
55
56
57
58
59
60

Plasma proteins including fibrinogen and albumin adsorb easily to the material surface through nonspecific interactions, and the cell adhesion behavior depends strongly on the amount, the composition, and the structure of adsorbed proteins. Thus, its surface adsorption amount was analyzed by a micro BCA using PPP. The result is shown in

1
2
3
4 Figure 2. A significant change was observed for the adsorbed proteins from PPP onto
5
6
7 PMEA and H-PMEA, probably due to the effect of physical crosslinking that restrict the
8
9
10 mobility of polymer chains and reduces the amount of IWC. Even though H-PMEA
11
12
13 adsorbs more proteins than PMEA, their amount is much less than the ones adsorbed
14
15
16 onto PP and especially PVC.
17
18
19
20



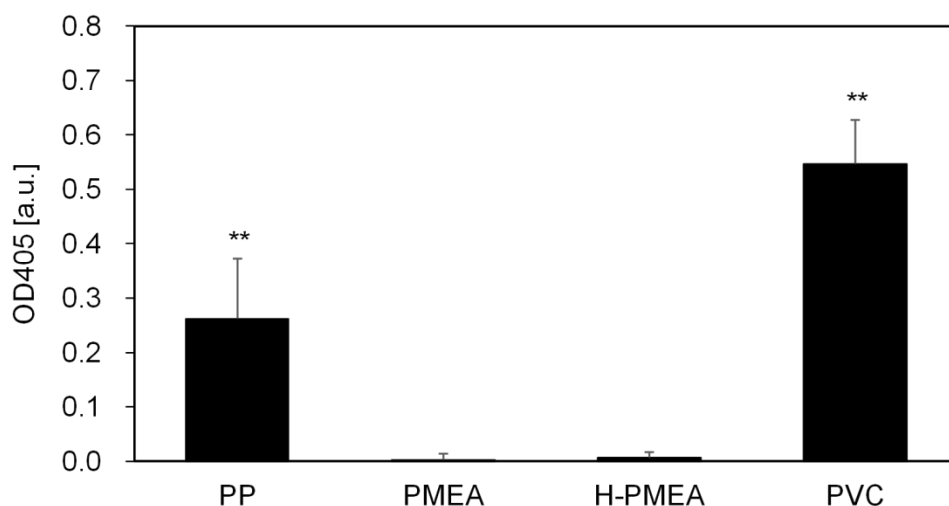
21
22
23
24
25
26
27
28
29
30
31
32
33
34
35
36
37 **Figure 2.** Amount of adsorbed proteins determined by the micro BCA method with PPP.

38 The data represent the mean \pm SD (n = 5). **: P < 0.01 vs. PMEA, and *: P < 0.05 vs.

39
40
41
42
43
44
45 PMEA. PP and PVC are used as controls.
46
47
48

49 Subsequently, the conformational alteration of adsorbed fibrinogen was quantified by
50
51
52 an ELISA. The plasma proteins change in conformation due to the contact with the
53
54
55
56
57
58
59
60

1
2
3
4 foreign body surface. The conformational alteration exposes the platelet adhesion site in
5
6
7 fibrinogen, and the exposure degree of this site on the material surface has a direct
8
9
10 impact on the non-thrombogenic property of materials. Thus, the ELISA with the
11
12
13 antibody that can identify c-terminus in the fibrinogen γ' chains – the platelet adhesion
14
15
16 site – was employed to evaluate the degree of the site exposure using PPP. The results
17
18
19
20
21 are presented in Figure 3. There was no significant difference between PMEA and H-
22
23
24 PMEA, and the conformation of adsorbed fibrinogen remained unchanged against the
25
26
27 adsorption onto both MEA polymer surfaces. In contrary, this is not the case for the
28
29
30
31 negative controls, PP and PVC, where even for PVC the conformational alteration of
32
33
34
35 fibrinogen is almost doubled as compared to PP (Figure 4).
36
37



1
2
3 **Figure 3.** Conformationally altered fibrinogen in the adsorbed proteins evaluated by the
4
5
6
7 ELISA method with PPP detected with an anti-fibrinogen γ' chain antibody after 1 h. The
8
9
10 data represent the mean \pm SD (n = 5). **: P < 0.01 vs. PMEA. PP and PVC are used as
11
12
13
14 controls.
15
16
17
18
19
20

21 **Analyses with human blood**

22
23
24 Platelet adhesion test with human blood is the best direct method to reveal the blood
25
26 compatibility of polymers. As depicted in Figure 4, the blood compatibility of H-PMEA is
27
28 slightly decreased as compared to that of PMEA, probably due to its higher hydrophobicity,
29
30 lower water and *IW* content, and chain mobility. Also, the free volume of the polymers is
31
32 expected to play a role, as the H-bonding should reduce the distances between 2 sliding
33
34 macromolecules. However, the decrease of the platelet adhesion on both MEA polymers as
35
36 compared to PET and PVC is enormous. These results further substantiate the anticipated big
37
38 advantage of the examined H-PMEA over the other hydrophobic polymers used as negative
39
40 control (Figure 2-4).
41
42
43
44
45
46
47
48
49
50
51
52
53
54
55
56
57
58
59
60

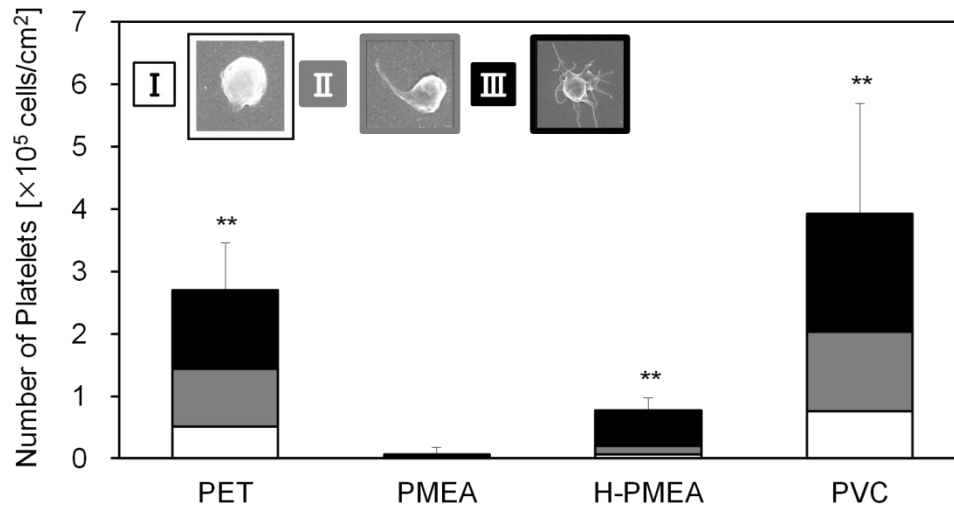
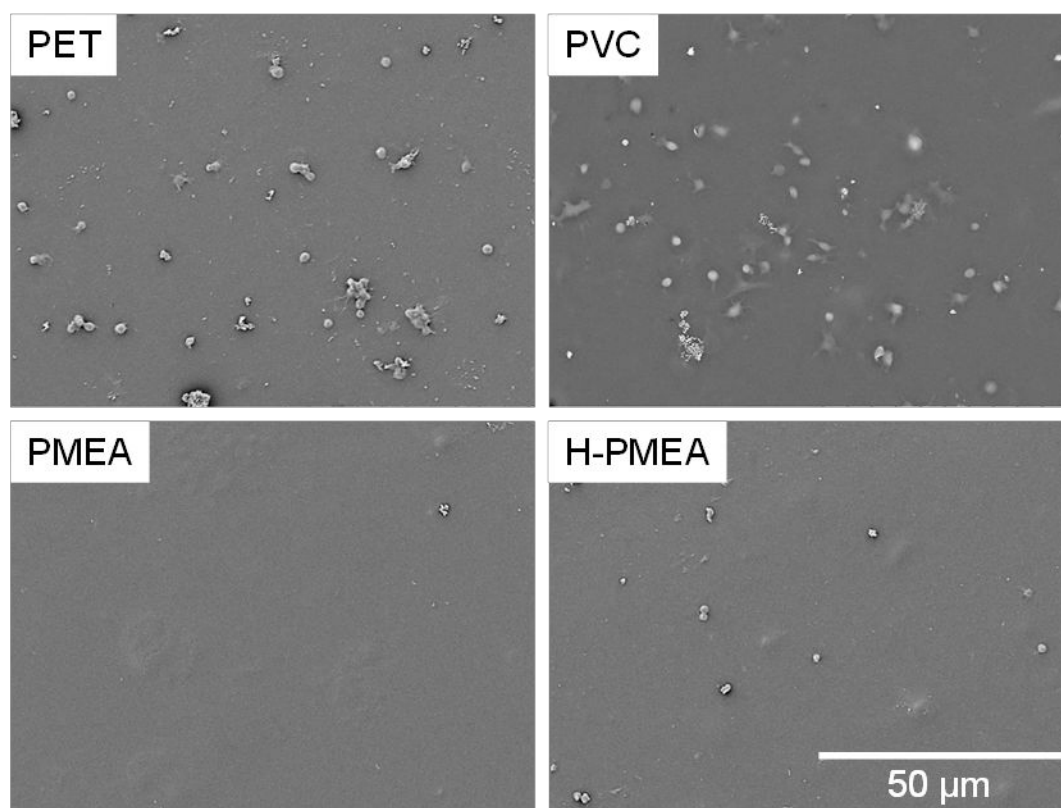


Figure 4. Platelet adhesion test with human blood onto PMEA and H-PMEA as compared to PET and PVC. Blood of three donors was tested in triplicates, and five fields were analyzed per substrate. The data represent the mean \pm SD. **: $P < 0.01$ vs. PMEA. PP and PVC were used as controls. The number of adhered platelets was classified into three types according to the degree of activation as shown in the figure: (I) native (spherical shape), (II) partially activated (hemispherical shape with several pseudopods), and (III) activated (spread shape with numerous pseudopods or flat discoid).

The morphology of the platelets (Figure 4) was observed by SEM (Figure 5). The platelet adhesion was suppressed by both PMEA and H-PMEA films onto PET,

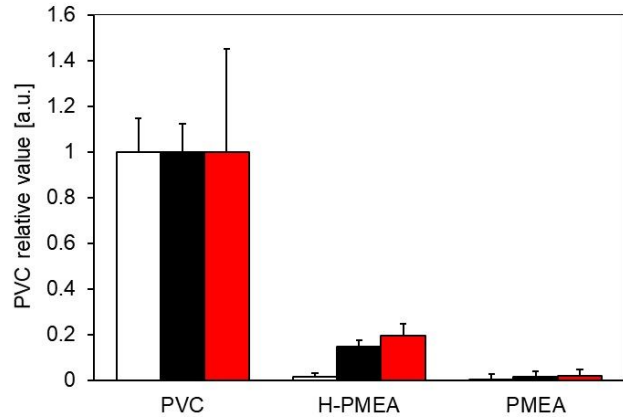
1
2
3 compared with that of untreated PET and PVC. The adhered platelets on all surfaces
4
5
6
7 except PME A formed many pseudopods and spread, which means that even though
8
9
10 there was a low number onto H-PMEA film, more than half of the platelets were highly
11
12
13
14 activated. PET and PVC have much higher numbers of adhered platelets, 33 and 48 %
15
16
17 of which show the highest activation degree III.
18
19
20
21
22
23



1
2
3 **Figure 5.** Scanning electron micrographs of platelets adhered onto the surface of PET,
4
5
6
7 PMEA, H-PMEA, and PVC. The scale bare corresponds to 50 μm in all micrographs.
8
9

10
11
12
13
14
15 The trend for the platelet compatibility of the MEA polymers evaluated in this work is
16
17
18 the same in all methods employed: ELISA, micro BCA, and human blood test.
19
20
21
22 Normalized values of the protein adsorption of the MEA polymers to that of PVC,
23
24
25 presented in Figure 6, suggest that the most blood compatible is PMEA, followed by H-
26
27
28 PMEA. In this order, the water content of the polymers and their IWC, as well as the
29
30
31
32 mobility and the hydrophilicity decreases, which explains the slightly decreased blood
33
34
35
36 compatibility of H-PMEA. This observation is in accord with the morphology/topography
37
38
39 of hydrated PMEA and H-PMEA obtained by AFM. Presence of more polymer-rich
40
41
42 protrusions and less water-rich valleys in hydrated H-PMEA results in H-PMEA being
43
44
45
46 slightly less blood compatible than PMEA as the protrusions are believed to serve as
47
48
49 scaffolds for fibrinogen (a protein playing an important role in thrombus formation)
50
51
52
53 adsorption and the valleys are expected to comprise much of W .³⁴⁻³⁶ Therefore, these
54
55
56
57
58
59
60

1
2
3 parameters can be used as a quantitative guidepost for the blood compatibility of
4
5
6
7 various materials.
8
9



10
11
12
13
14
15
16
17
18
19
20
21
22
23
24
25
26
27 **Figure 6.** Normalized values of the conformational alteration of adsorbed fibrinogen
28
29
30 evaluated by ELISA (white), the amount of adsorbed protein from PPP evaluated by μ -
31
32
33
34 BCA (black), and the number of adhered platelets by human platelet adhesion test (red)
35
36
37 to those of PVC.
38
39

40
41
42 Despite slight decrease in blood compatibility, the gain from turning the viscous PMEA
43
44
45 to solid H-PMEA is enormous: preparation of free-standing films, thick coatings,
46
47
48 possibly articles with various shapes and geometries for the medicinal and anti-fouling
49
50
51
52 industry with still significantly higher compatibility with human blood as compared to
53
54
55
56 PVC.
57
58
59
60

Conclusion

In conclusion, introducing strongly-associating hydrogen-bonding stickers in PMEA resulted in transforming this low viscosity polymer featuring excellent blood compatibility into a solid, rubber-like, and thermally stable supramolecular copolymer H-PMEA. Blood compatibility is assessed by 3 methods showing either no or slightly increased adsorption of platelets onto the rubbery H-PMEA when comparing it with the low viscosity PMEA. These changes in case of H-PMEA may be attributed to its higher hydrophobicity, lower chain mobility in hydrated condition, lower water, FW , and IW content as compared to the MEA homopolymer. Analysis of the free volume of both MEA polymers, which should also influence the water-polymer interactions at the interface, is being carried out. While sacrificing a bit the blood/platelet compatibility of PMEA, H-PMEA allows for the preparation of free-standing films and thick coatings as well as potentially tubes and articles with various shapes and geometries for the medicinal and anti-fouling industry with still significantly higher compatibility with human blood as compared to PVC. Thus, H-PMEA displays promising properties as the material that may replace polymers in products used in contact with blood or storage of

1
2
3 blood, which either are expensive or are known to comprise harmful for our health
4
5
6
7 compounds. The period of implementation during storage and processing can be at the
8
9
10 same time extended, the platelet adhesion dramatically suppressed, and the material
11
12
13 recycled. This strategy will be implemented in our laboratories to turn other viscous
14
15
16
17 blood compatible polymers into solid materials as well.
18
19
20
21
22
23

24 **ASSOCIATED CONTENT**

25 26 27 28 **Supporting Information**

29
30
31
32
33 Supporting Information. ^1H NMR spectroscopy, TGA, and DSC results for the
34
35
36 discussed polymers.
37
38
39

40
41 The Supporting Information is available free of charge on the ACS Publication
42
43
44 website at DOI: ***.
45
46
47

48 **AUTHOR INFORMATION**

49 50 51 52 **Corresponding Author**

53
54
55
56
57
58
59
60

1
2
3
4 *E-mail: masaru_tanaka@ms.ifoc.kyushu-u.ac.jp
5
6

7
8 **ORCID**
9

10
11
12 Katja Jankova: 0000-0002-4218-064X
13

14
15
16 Irakli Javakhishvili: 0000-0003-3681-3161
17

18
19
20 Shingo Kobayashi: 0000-0002-8357-8654
21
22

23
24
25 Ryohei Koguchi: 0000-0003-0017-4783
26
27

28
29
30 Daiki Murakami: 0000-0002-5552-4384
31
32

33
34
35 Toshiki Sonoda: 0000-0002-0504-7559
36
37

38
39
40 Masaru Tanaka: 0000-0002-1115-2080
41
42

43
44
45 **Notes**
46

47
48
49 The authors declare no competing financial interest.
50
51
52
53
54
55
56
57
58
59
60

ACKNOWLEDGEMENTS

Project PROGRESS 100 from Kyushu University is acknowledged for financial support. This work was partially supported by Dynamic Alliance for Open Innovation Bridging Human, Environment and Materials.

REFERENCES

- (1) Tanaka, M.; Motomura, T.; Kawada, M.; Anzai, T.; Kasori, Y.; Shiroya, T.; Shimura, K.; Onishi, M.; Mochizuki, A. Blood compatible aspects of poly(2-methoxyethylacrylate) (PMEA) – relationship between protein adsorption and platelet adhesion on PMEA surface. *Biomaterials* **2000**, *21* (14), 1471–1481.
- (2) Tanaka, M.; Motomura, T.; Kawada, M.; Anzai, T.; Kasori, Y.; Shimura, K.; Onishi, M.; Mochizuki, A.; Okahaya, Y. A new blood-compatible surface prepared by poly(2-methoxyethylacrylate)(PMEA) coating-protein adsorption on PMEA surface. *Jpn. J. Artif. Organs* **2000**, *29*, 209-216.
- (3) Tanaka, M.; Mochizuki, A.; Ishii, N.; Motomura, T.; Hatakeyama, T. Study of Blood Compatibility with Poly(2methoxyethyl acrylate). Relationship between Water Structure and Platelet Compatibility in Poly(2-methoxyethyl acrylate-co-2-hydroxyethyl methacrylate). *Biomacromolecules* **2002**, *3* (1), 36–41.

- 1
2
3 (4) Anzai, T.; Okumura, A.; Kawaura, M.; Yokoyama, K.; Oshiyama, H.; Kido, T.; Nojiri, C.
4 Evaluation of the Biocompatibility of an In Vitro Test Using a Poly(2-
5 methoxyethylacrylate) Coated Oxygenator. *Jpn. J. Artif. Organs* **2000**, *9*, 73-77.
6
7
8
9
10 (5) Lee, W.; Kobayashi, S.; Nagase, M.; Jimbo, Y.; Saito, I.; Inoe, Y.; Yambe, T.; Sekino, M.;
11 Malliaras, G.G.; Yokota, T.; Tanaka, M.; Someya, T. Nontrombogenic, stretchable, active
12 multielectrode array for electroanatomical mapping. *Science Advances* **2018**, *4*:eaau2426.
13
14
15
16
17 (6) Murakami, D.; Mawatari, N.; Sonoda, T.; Kawazaki, A.; Tanaka, M. Effect of the
18 molecular weight of Poly(2-methoxyethyl acrylate) on Interfacial Structure and Blood
19 Compatibility. *Langmuir* **2019**, *35*, 2808-2813.
20
21
22
23
24 (7) Kureha, T.; Hiroshige, S.; Matsui, S.; Suzuki, D. Water-immiscible bioinert coatings and
25 film formation aqueous dispersions of poly(2-methoxyethyl acrylate) microspheres.
26
27
28
29
30
31
32
33 (8) Bottehuis, N.E.; van Beek, D.J.M.; van Gemert, G.M.L.; Bosman, A.W.; Sijbesma, R.P.
34 Self-assembly and morphology of polydimethylsiloxane supramolecular thermoplastic
35 elastomers, *J. Polym. Sci., Part A: Polym. Chem.* **2008**, *46* (12), 3877-3885.
36
37
38
39 (9) Yamauchi, K.; Lizotte, J.R.; Long, T.E. Thermoreversible poly(alkyl acrylates) consisting
40 of self-complementary multiple hydrogen bonding. *Macromolecules* **2003**, *36* (4), 1083-
41 1088.
42
43
44
45
46
47 (10) Oglioni, E.; Yu, L.; Javakhishvili, I.; Skov, A.L. A thermo-reversible silicone elastomer
48 with remotely controlled self-healing. *RSC Adv.* **2018**, *8*, 8285-8291.
49
50
51
52 (11) Chen, S.; Mahmood, N.; Beiner, M.; Binder, W.H. Self-Healing Materials from V- and
53 H-Shaped Supramolecular Architectures. *Angew. Chem. Int. Ed.* **2015**, *54*, 10188–10192
54
55
56
57
58
59
60

- 1
2
3 (12) Kajita, T.; Noro, A.; Mtsushita, Y. Design and properties of supramolecular elastomers.
4
5 *Polymer* **2017**, *128*, 297-310.
6
7
8 (13) Weber, M.J.; Dankers, Y.W. Supramolecular hydrogels for biomedical applications.
9
10 *Macromol. Biosci.* **2019**, *19*, 1800452.
11
12
13 (14) Pan, Y.; Hu, J.; Yang, Z.; Tan, L. From Fragile Plastic to Room-Temperature Self-
14
15 Healing Elastomer: Tuning Quadruple Hydrogen Bonding Interaction through One-Pot
16
17 Synthesis. *ACS Appl. Polym. Mater.* **2019**, DOI:10.1021/acsapm.8b00153
18
19
20 (15) Dimitrov, I.; Jankova, K.; Hvilsted, S. Synthesis of Polystyrene-Based Random
21
22 Copolymers with Balanced Number of Basic or Acidic Functional Groups. *J. Polym. Sci.,*
23
24 *Part A: Polym. Chem.* **2010**, *48*, 2044–2052.
25
26
27 (16) Kerres, J.; Ullrich, A.; Haring, T.; Baldauf, M.; Gebhardt, U.; Preidel, W. Preparation,
28
29 characterization and fuel cell application of new acid-base blend membranes. *J. New Mater.*
30
31 *Electrochem. Syst.* **2000**, *3* (3), 2000, 229-239.
32
33
34 (17) Li, W.; Manthiram, A.; Guiver, M.D. Acid-base blend membranes consisting of
35
36 sulfonated poly(ether ether ketone) and 5-amino-benzotriazole tethered polysulfone for
37
38 DMFC. *J. Membrane Sci.* **2010**, *362*, 289-297.
39
40
41 (18) Hietala, S.; Mononen, P.; Strandman, S.; Järvi, P.; Torkkeli, M.; Jankova, K.; Hvilsted,
42
43 S.; Tenhu, H. Synthesis and rheological properties of an associative star polymer in
44
45 aqueous solutions. *Polymer* **2007**, *48*, 4087–4096.
46
47
48 (19) Hietala, S.; Strandman, S.; Järvi, P.; Torkkeli, M.; Jankova, K.; Hvilsted, S.; Tenhu, H.
49
50 Rheological Properties of Associative Star Polymers in Aqueous Solutions: Effect of
51
52 Hydrophobe Length and Polymer Topology. *Macromolecules* **2009**, *42* (5), 1726–1732.
53
54
55
56
57
58
59
60

- 1
2
3 (20) Jankova, K.; Jannasch, P.; Hvilsted, S. Ion conducting solid polymer electrolytes based
4 on polypentafluorostyrene-*b*-polyether-*b*-polypentafluorostyrene prepared by atom transfer
5 radical polymerization *J. Mater. Chem.* **2004**, *14*, 2902-2908.
6
7
8
9
10 (21) Jannasch, P. Ionic conductivity in physical networks of polyethylene-polyether-
11 polyethylene triblock copolymers *Chem. Mater.* **2002**, *14*, 2718–2724.
12
13
14
15 (22) Haishima, Y.; Kawakami, T.; Fukui, C.; Tanoue, A. Characterization of alternative
16 plasticizers in poly(vinyl chloride) sheets for blood containers. *J. Vinyl Addit. Techn.* **2015**,
17 *22* (4), 520-528.
18
19
20
21
22
23 (23) www.renolit.com: Blood and blood component applications.
24
25
26 (24) www.melitek.com; www.pvcfreebloodbag.eu: New PVC-free blood bags have reached a
27 major milestone, **2015**.
28
29
30
31 (25) Bhaskaran Nair, C.S.; Vidya, R.; Ashalatha, P.M. Hexamoll DINCH plasticised PVC
32 containers for the storage of platelets. *Asian J. Transfus. Sci.* **2011**, *5*, 18-22.
33
34
35
36 (26) Dumont, L.J.; VandenBroeke, T. Seven-day storage of apheresis platelets: report on an in
37 vitro study. *Transfusion* **2003**, *43*, 143-150.
38
39
40
41 (27) Tanaka, M.; Mochizuki, A. Effect of water structure on blood compatibility - thermal
42 analysis of water in poly(meth)acrylate. *J. Biomed. Mater. Res.* **2004**, *68A* (4), 684–695.
43
44
45
46 (28) Sato, K.; Kobayashi, S.; Sekishita, A.; Wakui, M.; Tanaka, M. *Biomacromolecules* **2017**,
47 *18*, 1609-1616.
48
49
50
51 (29) Shabbir, A.; Javakhishvili, I.; Cervený, S.; Hvilsted, S.; Skov, A.L.; Hassager, O.;
52 Alvarez, N. Linear Viscoelastic and Dielectric Relaxation Response of Unentangled UPy-
53 Based Supramolecular Networks. *Macromolecules* **2016**, *49*, 3899-3910.
54
55
56
57
58
59
60

- 1
2
3 (30) Koguchi, R.; Jankova, K.; Tanabe, N.; Amino, Y.; Hayasaka, Y.; Kobayashi, D.;
4 Miyajima, T.; Yamamoto, K.; Tanaka, M. Controlling the hydration structure with small
5 amount of fluorine to produce blood compatible fluorinated poly(2-methoxyethyl acrylate).
6
7 *Biomacromolecules*, **2019**, *20*, 2265-2275.
8
9
10
11
12 (31) Kobayashi, S.; Wakui, M.; Iwata, Y.; Tanaka, M. Poly(ω -methoxyalkyl acrylate)s:
13 Nonthrombogenic Polymer Family with Tunable Protein Adsorption. *Biomacromolecules*
14 **2017**, *18* (12), 4214-4223.
15
16
17
18
19 (32) Sato, K.; Kobayashi, S.; Sekishita, A.; Wakui, M.; Tanaka, M. Synthesis and
20 Thrombogenicity Evaluation of Poly(3-methoxypropionic acid vinyl ester): A Candidate
21 for Blood-Compatible Polymers. *Biomacromolecules* **2017**, *18* (5), 1609–1616.
22
23
24
25
26 (33) Kajita, T.; Noro, A.; Matsushita, Y. Design and properties of supramolecular elastomers.
27 *Polymer* **2017**, *128*, 297-310.
28
29
30
31
32 (34) Murakami, D.; Kobayashi, S.; Tanaka, M. Interfacial Structures and Fibrinogen
33 Adsorption at Blood- Compatible Polymer/Water Interfaces. *ACS Biomater. Sci. Eng.* **2016**,
34 *2* (12), 2122–2126.
35
36
37
38
39 (35) Murakami, D.; Kitahara, Y.; Kobayashi, S.; Tanaka, M. Thermosensitive Polymer
40 Biocompatibility based on Interfacial Structure at Biointerface, *ACS Biomater. Sci. Eng.*
41 **2018**, *4*, 1591-1597.
42
43
44
45
46 (36) Ueda, T.; Murakami, D.; Tanaka, M. Analysis of interaction between interfacial structure
47 and fibrinogen at blood-compatible polymer/water interface. *Front. Chem.* **2018**, *6*, 542:
48 doi: 10.3389/fchem.2018.00542.
49
50
51
52
53
54
55
56
57
58
59
60

Table of content graphics

